Dissociation conditions and Raman spectra of CO2 + SO2 and CO2 + H2S hydrates

Chen, Litao; Lu, Hailong; Ripmeester, John A.

Publisher's version / Version de l'éditeur:
https://doi.org/10.1021/acs.iecr.5b00350
Industrial and Engineering Chemistry Research, 54, 21, pp. 5543-5549, 2015-05-05

I&EC research
Industrial & Engineering Chemistry Research

Article

pubs.acs.org/IECR

Dissociation Conditions and Raman Spectra of CO_2 + SO_2 and CO_2 + H_2S Hydrates

Litao Chen,[†] Hailong Lu,[‡] and John A. Ripmeester*

Steacie Institute for Molecular Sciences, National Research Council Canada, Ottawa, ON K1A 0R6, Canada

ABSTRACT: To further define the information needed for CO_2 gas sequestration and storage in the presence of impurities, the stability of hydrates made from CO_2 + SO_2 and CO_2 + H_2S mixtures was measured by an isochoric dissociation method. The hydrates were characterized with powder X-ray diffraction, confirming that CO_2 + SO_2 formed a structure I hydrate. The Raman spectra of CO_2 + SO_2 and CO_2 + H_2S hydrates were also measured along with those of THF + CO_2 + SO_2 and THF + CO_2 + H_2S hydrates to observe and assign the Raman peaks of SO_2 or H_2S in the small cages. It was found the SO_2 Raman peaks are at 1147.1 and 1155.4 cm^{-1} in large and small cages, respectively; the H_2S Raman peaks are at 2594.0 and 2603.0 cm^{-1} in large and small cages, respectively. At the equilibrium points established, the composition of the released gas mixture was analyzed by gas chromatography. Measurements for gas pressures (ranging from 0.72 to 3.59 MPa) and gas compositions (ranging from 0.04% to 7.63%, mole fraction of SO_2 or H_2S) at specific temperatures (ranging from 263.15 to 283.15 K) are reported. The SO_2 and H_2S impurities tend to stabilize the mixed CO_2 hydrates formed, with almost all of the impurity gases reporting with the hydrate phase at low concentrations.

INTRODUCTION

Carbon dioxide, as an important greenhouse gas, is thought to play a significant role in global climate change. The major source of CO_2 is fossil fuel combustion with emissions that have increased dramatically over the past few decades and for which about 43% of the CO_2 remains in the atmosphere.[1] A variety of technologies has been developed for the separation and capture of CO_2 from flue gas. Among these methods, hydrate formation (forming CO_2 hydrate to separate CO_2 from other gases) is promising because of the huge gas storage capacity of hydrates.[2] One volume of CO_2 hydrate can store ~160 volumes of CO_2 under standard conditions. Therefore, detailed equilibrium conditions of CO_2 hydrates are needed for developing CO_2 gas capture technologies.[3] The major components of flue gas are N_2 and CO_2, with O_2, NO_x, CO, and SO_2 as minor constituents. Among these components, the N_2 and O_2 hydrate formation pressures are much higher than those for CO_2. The SO_2 hydrate formation pressure is much lower than that for CO_2 hydrate.[4] Although SO_2 can be removed by other methods, hydration of CO_2 with SO_2 impurities may be more economically competitive compared to other methods.[5] Therefore, assessments on the influence of SO_2 on CO_2 hydrate stability are needed. Some assessment work has been done recently. Daraboina et al.[6] measured the hydrate equilibrium conditions of a CO_2−N_2−SO_2 mixture by using the isothermal pressure search method. They found the presence of SO_2 enhanced initial hydrate formation. Beeskow-Strauch et al. reviewed the properties of CO_2 hydrate and SO_2 hydrate.[5] They studied the stability of CO_2 hydrate with 1% SO_2 (mole fraction). However, only three stability data points for CO_2−SO_2 hydrate were measured by microscopic observation. Kim et al. measured the phase equilibria of hydrate formed from a CO_2 + SO_2 gas mixture (1% SO_2 and 10% SO_2, mole fraction).[7] The 1% SO_2 equilibrium data of Kim et al. fit well with that of Beeskow-Strauch et al. However, the data for the 10% SO_2 runs are dependent on the amount of water present, which is not unexpected for gas mixtures consisting of components with rather different solubilities. They assign the discrepancy to the different solubilities of CO_2 and SO_2 in water. With different amounts of water, the amount of SO_2 and CO_2 dissolved in water are quite different, so that the remaining gas mixture compositions also are different. However, in the two published papers, gas composition data (different from feed gas composition due to gas dissolution) under equilibrium conditions were not measured. In addition, more equilibrium data for various gas compositions over a larger temperature range are still needed.

Similar to that of SO_2, the influence of H_2S on the CO_2 hydrate stability will also be significant when CO_2 hydrate is sequestered underground in depleted natural gas reservoirs where H_2S may be present. H_2S hydrate was reported as early as 1840, forming a structure I (sI) hydrate with water,[8] and H_2S hydrate formation conditions have been reported in several publications.[9−11] Robinson and Hutton and Sun et al. measured the hydrate formation conditions of a CH_4 + CO_2 + H_2S gas mixture.[12,13] Nohra et al.[14] calculated the Gibbs free energy of the reactions of SO_2, CH_4, and H_2S substituting CO_2 in hydrate. The results show that SO_2 and H_2S should be able to substitute for CO_2 molecules in hydrate cages and also stabilize the hydrate. Nevertheless, neither phase equilibrium data nor the Raman spectrum for the binary hydrate (CO_2 + H_2S) has been reported to date.

Even small amounts of either SO_2 or H_2S present in CO_2 can modify the pressures and temperatures required to form a hydrate. However, software such as CSMGem, Multiflash, Hydrafact, etc. cannot predict the equilibrium conditions of the

Received: January 26, 2015
Revised: April 15, 2015
Accepted: May 5, 2015
Published: May 5, 2015

DOI: 10.1021/acs.iecr.5b00350
Ind. Eng. Chem. Res. 2015, 54, 5543−5549

CO_2 + SO_2 hydrate because of the lack of data for validation. More experimental data are needed to validate modeling. For the H_2S + CO_2 hydrate, more data are also needed to improve the accuracy of model prediction. In this work, stabilities of the hydrates formed from CO_2 + SO_2 and CO_2 + H_2S mixtures were studied. Hydrate dissociation equilibrium conditions were measured by the isochoric dissociation method with which the gas mixture composition at equilibrium is measured. In addition to the equilibrium conditions, the structure of the hydrate samples was studied by powder X-ray Diffraction (PXRD) and Raman spectroscopy. Raman spectra of CO_2 + SO_2, CO_2 + H_2S, THF + CO_2 + SO_2, and THF + CO_2 + H_2S hydrates are reported. Raman peaks of SO_2 and H_2S in small and large hydrate cages were assigned, and Raman spectra of CO_2 and SO_2 in different states were also reported.

EXPERIMENTAL SECTION

Material. CO_2 and SO_2 with the purity of 99.9% and H_2S with the purity of 99% were purchased from Praxair. Tetrahydrofuran (no stabilizer) with a purity of 99.9% and water (HPLC) were purchased from EMD Millipore.

Experimental Procedure. First, hydrate samples were synthesized in a 300 mL stainless steel autoclave. The detailed procedure is as follows: (i) 30 g of ice (or THF hydrate) powder was prepared by grinding ice or THF hydrate under liquid nitrogen. The powders were sieved keeping the 120 and 70 mesh fraction for hydrate formation. THF hydrate was formed by freezing a THF + H_2O (1:17 mol ratio) solution in liquid nitrogen. (ii) The autoclave was embedded in dry ice (194.7 K) in advance of loading. After the frozen powders were loaded, the autoclave was sealed, connected to a vacuum line, and evacuated. (iii) An appropriate amount of SO_2 or H_2S was measured and let into the autoclave by means of the vacuum line. Specifically, a bulb of known volume attached to the vacuum line was charged with the required amount of SO_2 or H_2S to a calculated pressure (less than 1 atm) to give the desired number of moles of gas, then the valve between the bulb and the autoclave was opened. SO_2 or H_2S then condensed in the autoclave which was placed in liquid nitrogen. The amount of SO_2 or H_2S needed was calculated from the amount of CO_2 at the various mole fractions (1%, 10%, or 50%) used. The 10% SO_2 + 90% CO_2 indicates the initial mole composition of the gas in total but not the composition in the gas phase as it evolves as hydrate forms. (iv) The autoclave was placed in a bath at 273 K to equilibrate for 30 min. Then we charged the autoclave with CO_2 gas to 3.2 MPa. The CO_2 gas, the amount of which is determined by pressure (3.2 MPa), volume, and temperature, was cooled by passing it through a coil immersed in a cooling bath to avoid the melting of the ice/THF hydrate powders. (v) After 7 days of reaction, the autoclave was cooled in liquid nitrogen and the hydrate sample was recovered and stored in several 25 mL sealed glass vials in liquid nitrogen for further use.

Hydrate equilibrium conditions were obtained by dissociating hydrate samples under isochoric and constant temperature conditions. This method was shown to be reliable for the phase boundary measurements of hydrate formed from gas mixtures.[15,16] The hydrate dissociation procedures are given below. First, a 10 mL stainless steel cylinder (immersed in liquid nitrogen) was filled with the previously synthesized hydrate sample. The cylinder was then evacuated in liquid nitrogen to remove air and sealed. Second, the cylinder was placed in a cooling bath (preset to the desired experimental temperature); the hydrate started to dissociate, and the pressure increased in the cylinder. Third, when the rate of pressure increase was less than 0.01 MPa/3 h, the system was taken to have reached equilibrium. The gas phase was then sampled and analyzed. The composition of the gas phase was analyzed by an SRI 8610C type gas chromatograph and a set of temperature−pressure−composition data was obtained. The bath temperature was then increased to a higher value, and a series of equilibrium condition data at different temperatures was obtained. A typical pressure−temperature−time profile for hydrate dissociation is shown in Figure 1.

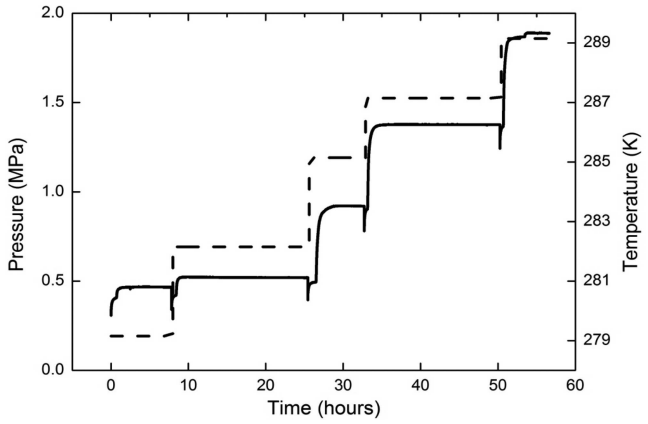

Figure 1. Typical pressure−temperature−time profile in the isochoric dissociation measurement. Solid line, pressure; dashed line, temperature.

Hydrate samples were characterized by PXRD and Raman spectroscopy. The PXRD measurements were performed in 2θ scan mode with a step width of 0.032° in the range of 8.0−49.8° using Cu Kα radiation (λ = 1.5406) at 120 K and ambient pressure (40 kV, 40 mA, Bruker AXS model D8 Advance). The PXRD pattern was Rietveld-refined by using the Fullprof suite.[17] A Raman spectrometer (Spectropro 2500i, Acton Research Corporation) equipped with a Witec confocal microscope and an Ar^+ laser (177G, wavelength 514.5 nm, Spectra-Physics) was used in this work. Raman measurements were performed at liquid nitrogen temperature. The spectrometer was calibrated with naphthalene before use. CO_2 hydrate equilibrium conditions were taken from the literature.[8]

RESULTS AND DISCUSSION

Powder X-ray diffraction results confirm the structure of CO_2 + SO_2 hydrate to be sI. Raman spectra of CO_2, SO_2, and H_2S in hydrate cages were also measured. It was found that the SO_2 Raman peaks are at 1147.1 and 1155.4 cm^{-1} in the large and small cage, respectively. The H_2S Raman peaks are at 2594.0 and 2603.0 cm^{-1} in the large and small cage, respectively. The dissociation conditions of CO_2 + SO_2 and CO_2 + H_2S hydrates were obtained by using the aforementioned isochoric dissociation method. A series of pressure−temperature−composition (T−P−C) data are reported, with gas compositions at equilibrium measured by GC. The hydrate formation/dissociation process and distillation effect is discussed.

Structure and Raman Spectra. *Powder X-ray Diffraction.* Figure 2 shows the PXRD result of SO_2 + CO_2 hydrate. It shows that mixed SO_2 + CO_2 hydrates are structure I. In

DOI: 10.1021/acs.iecr.5b00350
Ind. Eng. Chem. Res. 2015, 54, 5543−5549

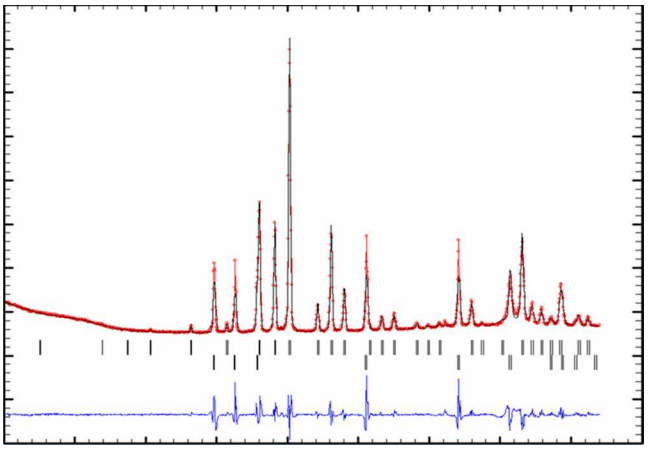

Figure 2. PXRD result of the SO_2 + CO_2 hydrate. Space group, $Pm\bar{3}n$; cell parameters, $a = b = c = 11.8559 \pm 0.0021$; structure I hydrate. Black line, measured profile; red dots, Rietveld-refined by Fullprof; blue line, difference between measured and fitted profile. Top black bars, sI hydrate; bottom black bars, ice.

addition to the sI hydrate, there is some ice Ih in the sample. The fractions of sI hydrate and ice Ih were about 0.74 and 0.26, respectively.

Figure 3 shows PXRD result of THF + CO_2 hydrate. It shows that THF + CO_2 hydrate is structure II (sII), as

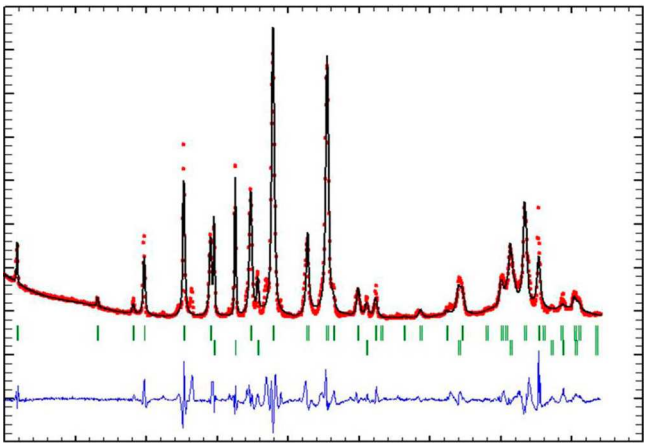

Figure 3. PXRD result of the THF + CO_2 hydrate. Space group, $Fd\bar{3}m$; cell parameters, $a = b = c = 17.2078 \pm 0.0021$; structure II hydrate. Black line, measured profile; red dots, Rietveld-refined by Fullprof; blue line, difference between measured and fitted profile. Top green bars, sII hydrate; bottom green bars, ice.

expected. There is also some Ih ice in the sample. The fractions of sII hydrate and ice Ih were about 0.66 and 0.34, respectively.

Raman Spectra. Raman spectroscopic measurements were performed on SO_2 + CO_2 hydrate, THF + CO_2 hydrate, THF + SO_2 + CO_2 hydrate, H_2S + CO_2 hydrate, and THF + H_2S + CO_2 hydrate.

SO_2 + CO_2 Hydrate. Figure 4 shows the spectra for SO_2 + CO_2 gas, CO_2 + SO_2 hydrate, and solid CO_2. In the SO_2 + CO_2 gas spectrum, peaks at 1285.1 cm $^{-1}$ and 1388.5 cm $^{-1}$ are assigned to the Fermi dyad characteristic of CO_2, and the peak at 1151.5 cm $^{-1}$ can be assigned to SO_2. The CO_2 + SO_2 gas spectrum agrees very well with the literature.[5,18] If CO_2 is present in the solid state, the Fermi dyad peaks shift to lower frequencies at 1276.3 and 1384.7 cm^{-1}. When SO_2 is

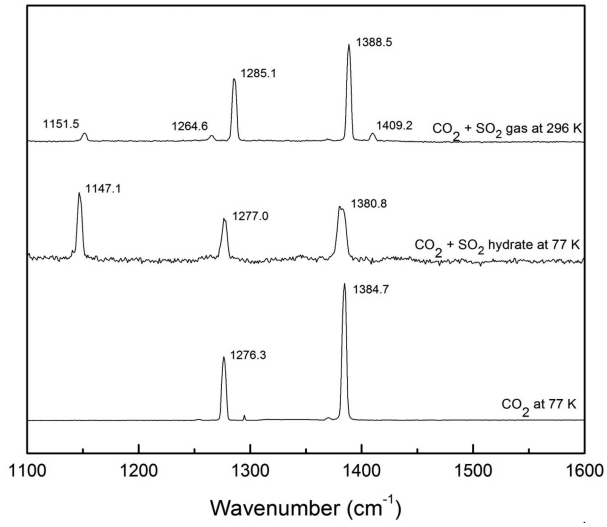

Figure 4. Raman spectra of CO_2 and SO_2 in different states. Gaseous CO_2, 1285.1 and 1388.5 cm^{-1}; solid CO_2, 1276.3 and 1384.7 cm^{-1}; CO_2 in sI hydrate, 1277.0 and 1380.8 cm^{-1}; SO_2 in large cage, 1147.1 cm^{-1}.

enclathrated, the peak at 1151.5 cm^{-1} shifts to a lower frequency at 1147.1 cm^{-1}. For enclathrated CO_2 the higher-frequency peak of the Fermi dyad blue shifts to 1380.8 cm^{-1}. The Raman peaks for CO_2 + SO_2 hydrate also agree very well with those in the literature.[5] There are two types of cages in CO_2 + SO_2 sI hydrate, a small cage (5^{12}) and a large cage ($5^{12}6^2$). Some Raman peaks have been observed to split to distinguish guests in small and large cages, allowing estimates of cage occupancies. For the Raman spectrum of CO_2 + SO_2 hydrate, splitting of the peaks is not observed for either CO_2 or SO_2. According to the intensity of the SO_2 peak in the CO_2 + SO_2 hydrate spectrum, the 1147.1 cm^{-1} peak should be assigned to SO_2 in the large cage. Although SO_2 can occupy both large and small cages in pure sI hydrate,[8] we think that SO_2 occupies only the large cage in the CO_2 + SO_2 hydrate because the observed peaks are not peaks attributable to SO_2 in small cages. CO_2 can occupy both large and small cages in sI, but spectra do not show splitting of the Fermi doublet. An explanation has been proposed in the literature.[19]

The spectra of THF + CO_2 hydrate and THF + SO_2 + CO_2 hydrate are shown in Figure 5. As shown in Figure 3, THF + CO_2 forms a sII hydrate. In sII THF + CO_2 hydrate, THF occupies all of the large cages while CO_2 occupies only some of the small cages; hence, the Fermi doublet frequencies in Figure 5 should be assigned to CO_2 in the small cage of sII hydrate. For THF + CO_2 + SO_2 hydrate, CO_2 occupies the small cage and the Fermi dyad peaks are at 1274.3 and 1380.5 cm^{-1}. Two peaks were observed for SO_2. According to the literature,[20,21] the peak for solid SO_2 is at 1148 cm^{-1}, so the peak at 1155.4 cm^{-1} must be for SO_2 in a hydrate cage. If the 1147 cm^{-1} peak is for SO_2 in the large cage, the 1155.4 cm^{-1} peak should be assigned to SO_2 in the small cage. Because SO_2 in the large cage is observed for the THF + CO_2 + SO_2 hydrate, we speculate that SO_2 replaces some THF in the large cage of sII hydrate or forms sI SO_2 hydrate.

H_2S + CO_2 Hydrate. The spectra of H_2S + CO_2 hydrate and THF + H_2S + CO_2 hydrate are shown in Figure 6. There are two peaks for H_2S in CO_2 + H_2S hydrate, at 2594.0 and 2606.3 cm^{-1}. The peak positions agree very well with values in the

DOI: 10.1021/acs.iecr.5b00350
Ind. Eng. Chem. Res. 2015, 54, 5543−5549

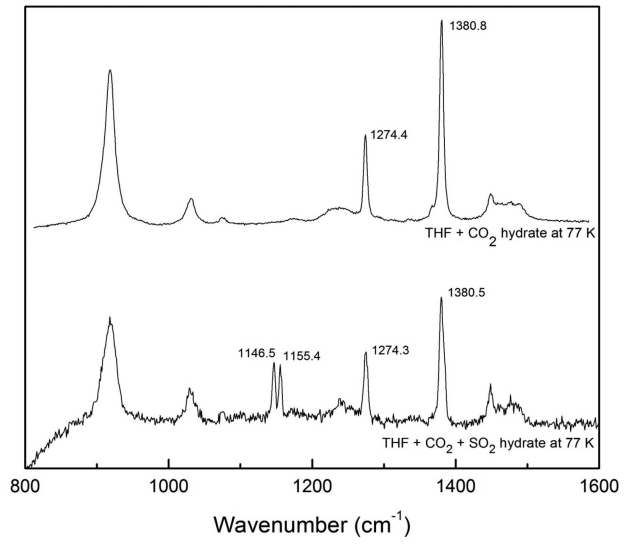

Figure 5. Raman spectrum of CO_2 and SO_2 in THF hydrate. CO_2 in small cage, 1274.4 and 1380.8 cm^{-1}; SO_2 in large cage, 1146.5 cm^{-1}; SO_2 in small cage, 1155.4 cm^{-1}.

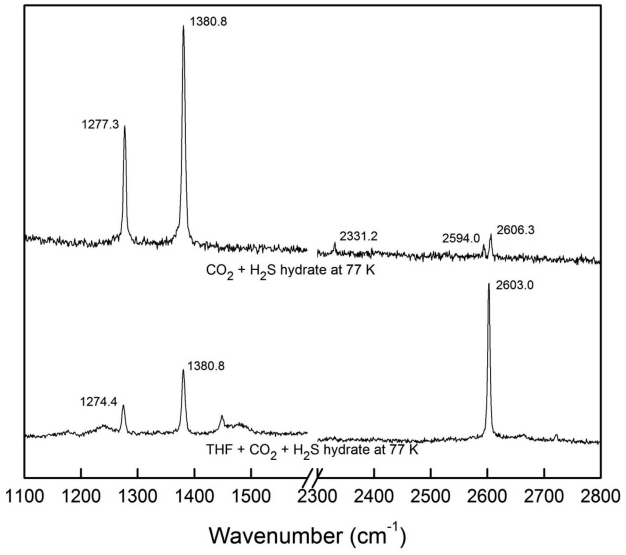

Figure 6. Raman spectra of binary CO_2 + H_2S hydrate and ternary THF + CO_2 + H_2S hydrate. H_2S in the large cage of sI hydrate, 2594.0 cm^{-1}; H_2S in the small cage of sI hydrate, 2606.3 cm^{-1}; H_2S in the small cage of sII hydrate, 2603.0 cm^{-1}; CO_2 in sI hydrate cages, 1277.3 and 1380.8 cm^{-1}; CO_2 in the small cage of sII hydrate, 1274.4 and 1380.8 cm^{-1}.

literature.[22] Also according to the literature,[23] the 2594.0 cm^{-1} peak should be assigned to H_2S in the large cage; therefore, the 2606.3 cm^{-1} peak should be assigned to H_2S in the small cage. This peak assignment was determined from the THF + H_2S + CO_2 hydrate spectrum. For THF + H_2S + CO_2 hydrate, we assume THF occupies all of the large cages while CO_2 and H_2S occupy the small cage. The peak at 2603.0 cm^{-1} should be assigned to H_2S in the small cage of sII hydrate. For the H_2S + CO_2 hydrate, it seems H_2S occupies both the small cage and the large cage because two peaks were observed (2594 and 2606 cm^{-1}). The CO_2 Fermi dyad peaks are in good agreement for all of the Raman spectra. For CO_2 in the sI large cage, for example, CO_2 + SO_2 hydrate and CO_2 + H_2S hydrate, the Fermi dyad peaks are at 1277 and 1381 cm^{-1}. For CO_2 in the sII small cage, for example, THF + CO_2 hydrate, THF + CO_2 + SO_2 hydrate, and THF + CO_2 + H_2S hydrate, the Fermi dyad peaks are at 1274 and 1381 cm^{-1}.

The Raman peak positions of SO_2 and H_2S in small and large cages are summarized in Table 1. According to the loose cage−tight cage model,[24,25] a larger cage leads to a lower frequency for the stretching vibration. From Table 1, we see that both SO_2 and H_2S follow the loose cage−tight cage model.

Table 1. Raman Signature of SO_2 and H_2S in Different Systems

sample and conditions	small cage	large cage
SO_2 in sI CO_2 + SO_2 hydrate, 77 K, 1 bar		1147.1 ± 1.0
SO_2 in sII THF + CO_2 + SO_2 hydrate, 77 K, 1 bar	1155.4 ± 1.0	1146.5 ± 1.0
H_2S in CO_2 + H_2S hydrate, 77 K, 1 bar	2606.3 ± 1.0	2594.0 ± 1.0
H_2S in THF + CO_2 + H_2S hydrate, 77 K, 1 bar	2603.0 ± 1.0	

Equilibrium Conditions. Dissociation conditions of hydrate formed from different feed gas compositions (1% SO_2 + 99% CO_2, 10% SO_2 + 90% CO_2, 50% SO_2 + 50% CO_2, 1% H_2S + 99% CO_2, and 10% H_2S + 90% CO_2) were measured. Both SO_2 and H_2S tend to decrease the equilibrium pressure of mixed CO_2 hydrate. The gas mixture compositions at equilibrium are reported together with the equilibrium temperature and pressure.

CO_2 + SO_2 Hydrate. Hydrate samples were synthesized from three CO_2 + SO_2 mixtures (SO_2 at 1%, 10%, and 50% mole fraction). Five measurements were performed, and 22 sets of equilibrium data points were obtained. The temperature range was (263.15−281.15) K, and the pressure range was (0.72−2.04) MPa. The highest SO_2 mole fraction in the released gas phase was 1.09%. The measured T−P−C data are listed in Table 2 and plotted in Figure 7. For comparison, literature data[5,7,8] for CO_2 hydrate and for the 1% SO_2 + 99% CO_2 hydrate are also plotted in Figure 7. The results show that the data in this work agree very well with the literature data. As shown in Figure 7, almost all of the measured pressures for the mixed hydrates are a little lower than those for the pure CO_2 hydrate. Clearly, SO_2 decreases the equilibrium pressure of the mixed hydrate, with the extent of the decrease determined by the fraction of SO_2. As listed in Table 2, the SO_2 fraction in the gas phase is very low (less than 0.35%) compared to that in the feed mixture, indicating that SO_2 is concentrated in the hydrate phase.

For the hydrates formed from the 10% SO_2 + 90% CO_2 and the 50% SO_2 + 50% CO_2 mixtures, the equilibrium pressures are appreciably lower than those for CO_2 hydrate. As shown in Table 2, the SO_2 fractions in the vapor phase for the hydrates formed from the 10% SO_2 + 90% CO_2 and 50% SO_2 + 50% CO_2 mixtures are somewhat higher than those for the hydrate formed from the 1% SO_2 + 99% CO_2 mixture. This observation follows the trend of the higher SO_2 fraction with a larger pressure decrease. If we look at the SO_2 fractional change in each run, we can see that the SO_2 fraction increases with temperature. At the same time, the pressure decrease (compared to CO_2 hydrate) increases as shown in Figure 7.

As shown in Table 2, the SO_2 fraction in the vapor phase is very small and reflects the greater affinity of SO_2 for the hydrate phase as compared to CO_2, as also evident from the decomposition pressures of the pure CO_2 and SO_2 hydrates. Under kinetic control, it is likely that most of the SO_2 in the gas

DOI: 10.1021/acs.iecr.5b00350
Ind. Eng. Chem. Res. 2015, 54, 5543−5549

Table 2. Dissociation Equilibrium Conditions of SO_2 + CO_2 Mixture-Formed Hydrate

sample	temperature (K)	pressure (MPa)	SO_2 (mole %)	CO_2 (mole %)	phases
1% SO_2 + 99% CO_2 in feed mixture, run 1	273.15	1.20	0.04	99.96	L_W−H−V
	275.15	1.52	0.04	99.96	L_W−H−V
1% SO_2 + 99% CO_2 in feed mixture, run 2	263.15	0.72	0.15	99.85	L_W−H−V
	266.15	0.80	0.15	99.85	L_W−H−V
	269.15	0.88	0.19	99.81	L_W−H−V
	272.15	1.06	0.16	99.84	L_W−H−V
	275.15	1.46	0.28	99.72	L_W−H−V
	278.15	1.89	0.34	99.66	L_W−H−V
1% SO_2 + 99% CO_2 in feed mixture, run 3	263.15	0.73	0.05	99.95	L_W−H−V
	266.15	0.81	0.08	99.92	L_W−H−V
	269.15	0.91	0.09	99.91	L_W−H−V
	272.15	1.08	0.05	99.95	L_W−H−V
	275.15	1.51	0.07	99.93	L_W−H−V
	278.15	2.04	0.10	99.90	L_W−H−V
10% SO_2 + 90% CO_2 in feed mixture	275.15	1.50	0.15	99.85	L_W−H−V
	277.15	1.86	0.23	99.77	L_W−H−V
	279.15	2.33	0.33	99.67	L_W−H−V
50% SO_2 + 50% CO_2 in feed mixture	273.15	1.17	0.26	99.74	L_W−H−V
	275.15	1.44	0.39	99.61	L_W−H−V
	277.15	1.73	0.62	99.38	L_W−H−V
	279.15	1.76	0.69	99.31	L_W−H−V
	281.15	1.85	1.09	98.91	L_W−H−V

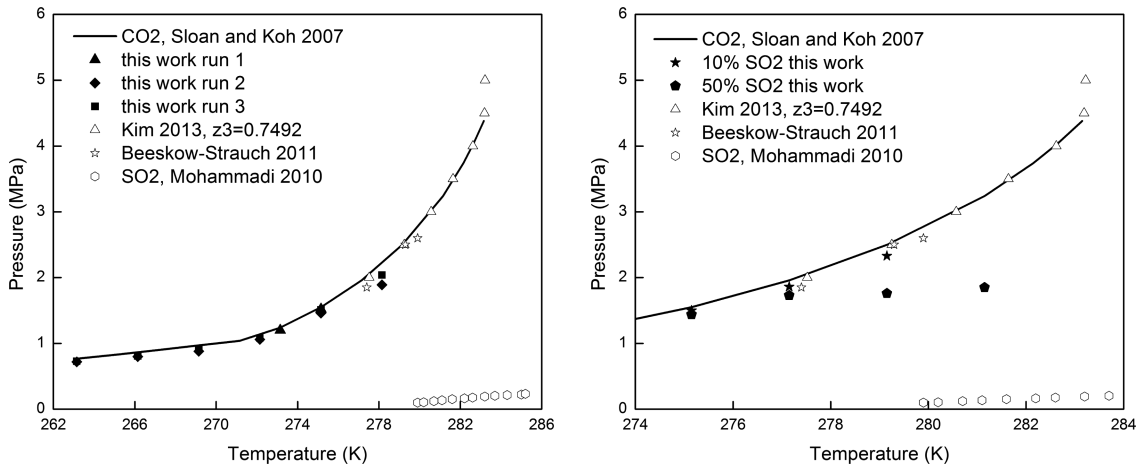

Figure 7. Dissociation conditions of hydrate formed from SO_2 + CO_2 mixture. Left panel: 1% SO_2 + 99% CO_2 feed mixture. Right panel: hydrates formed from 10% SO_2 + 90% CO_2 feed mixture and from 50% SO_2 + 50% CO_2 feed mixture. Solid line, CO_2 hydrate equilibrium conditions (ref 8); solid triangle, solid diamond, and solid cubic, 1% SO_2 + 99% CO_2 feed mixture (this work); solid star, 10% SO_2 + 90% CO_2 feed mixture (this work); solid pentagon, 50% SO_2 + 50% CO_2 feed mixture (this work); empty star, 1% SO_2 + 99% CO_2 feed gas (ref 5); empty triangle, 1% SO_2 + 99% CO_2 feed gas (ref 7), y = 0.1, z_3 = 0.7492; empty hexagon, SO_2 hydrate equilibrium conditions (ref 4).

mixture will react with ice to form hydrate in the early stages of the hydrate formation process, leaving the gas mixture depleted in SO_2. To reach the equilibrium composition, SO_2 would need to pass between the gas and solid phases a number of times. This is the distillation effect in hydrate formation. During the dissociation of an equilibrium CO_2 + SO_2 hydrate, both CO_2 and SO_2 are released. Initially this will enrich the gas mixture in SO_2, although because there is now a liquid phase present, most of the SO_2 will dissolve in the aqueous liquid. Both formation and dissociation processes are likely to be rather complex for SO_2 + CO_2 mixtures, especially at low concentrations of SO_2.

The phases that result from gas mixtures of different compositions can be determined by a flash calculation. At 273 K and 3.2 MPa, the 1% SO_2 + 99% CO_2 mixture is at V−L equilibrium and the 10% SO_2 + 90% CO_2 and 50% SO_2 + 50% CO_2 mixture are in the liquid phase. For the SO_2 + CO_2 hydrate experiment, most of the SO_2 + CO_2 mixture in the autoclave during hydrate formation is in the liquid phase and a smaller amount of SO_2 + CO_2 in the vapor phase. Hydrate may form from both the liquid and SO_2 + CO_2 vapor mixtures, and this likely will affect the kinetics of the formation process. However, with sufficient time it should not affect the dissociation equilibrium conditions as the thermodynamic properties are not changed by the amount of the components. According to the Gibbs phase rule, $F = C - P + 2$, the degrees of freedom for SO_2 + CO_2 hydrate at L_w−H−V equilibrium is 2 = 3 − 3 + 2. In our experiments, the temperature was held constant and the gas composition at equilibrium was measured directly. When the two degrees of freedoms are fixed, the equilibrium pressure should also be fixed. Therefore, there

DOI: 10.1021/acs.iecr.5b00350
Ind. Eng. Chem. Res. 2015, 54, 5543−5549

Table 3. Dissociation Equilibrium Conditions of the H_2S + CO_2 Mixture-Formed Hydrate[a]

sample	temp (K)	P_{exp} (MPa)	H_2S (mole %)	P_{CSMGem} (MPa)	ADP (%)	$P_{Multiflash}$(MPa)	AADP (%)
10% H_2S + 90% CO_2 in feed gas	278.15	1.82	2.67	1.41	22.53	1.59	12.64
	281.15	2.21	3.76	1.79	19.00	2.02	8.60
	284.15	2.29	7.63	1.88	17.90	2.10	8.30
average					19.81		9.84
1% H_2S + 99% CO_2 in feed gas	263.15	0.73	0.20	0.71	2.74	0.75	2.74
	268.15	0.87	0.49	0.81	6.90	0.88	1.15
	273.15	1.16	0.67	1.05	9.48	1.13	2.59
	278.15	2.06	1.17	1.73	16.02	1.88	8.74
	283.15	3.59	1.85	2.89	19.50	3.22	10.31
average					10.93		5.10
total					14.26		6.88

[a]All are at L_W−H−V equilibrium.

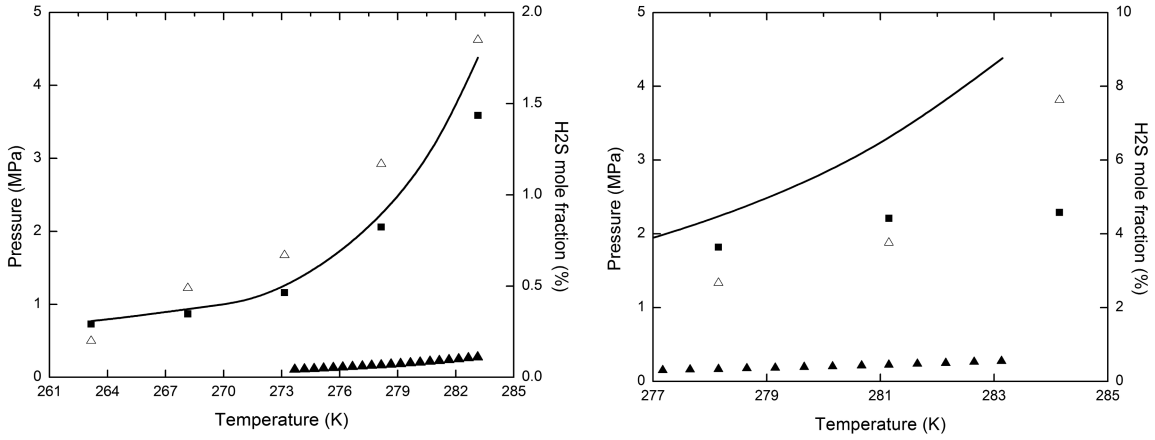

Figure 8. Dissociation conditions of hydrate formed from H_2S + CO_2 gas mixture. Left panel: 1% H_2S + 99% CO_2 feed gas. Right panel: 10% H_2S + 90% CO_2 feed gas. Solid line, CO_2 hydrate equilibrium conditions (ref 8); empty triangles, H_2S mole fraction in gas phase (this work); solid cube, equilibrium pressure (this work); solid triangle, H_2S hydrate equilibrium conditions (ref 11).

should be only one equilibrium pressure at a determined gas composition and temperature, and the measured data can be considered to be reliable.

The amount of ice powder also cannot change the equilibrium conditions. More ice will consume more CO_2 or SO_2, forming more hydrate, and the liquid and gas composition should change to reach new equilibrium. The equilibrium pressure is determined by the gas composition and temperature and should be independent of the amount of ice powder. Because of the solubility difference of CO_2 and SO_2 in water, the amount of hydrate (water) should affect the gas mixture composition. In ref 7, the measured equilibrium pressure is different in different water fraction experiments. We think the reason is the amount of dissolved SO_2 is different in different water fraction experiments. The feed gas mixture composition is fixed at 10% SO_2 + 99% CO_2. If the dissolved SO_2 amounts are different, the remaining gas mixture compositions are different. The measured equilibrium conditions are actually for different SO_2 + CO_2 compositions. However, in this work, we measure the gas mixture composition directly at equilibrium. The influence of solubility difference has been removed. So the hydrate amount (ice/water amount) does not affect the equilibrium conditions.

H_2S + CO_2 Hydrate. CO_2 + H_2S hydrate was synthesized from 1% H_2S + 99% CO_2 and 10% H_2S + 90% CO_2 feed gas mixtures. The 1% H_2S + 99% CO_2 and 10% H_2S + 90% CO_2 mixtures are both present as vapors at 273 K and 3.2 MPa. Two sets of measurements were performed, and eight sets of data were obtained. The temperature range was (263.15 to 287.15) K, and the pressure range was (0.73 to 3.59) MPa. The highest H_2S mole fraction was 7.63%. The data are listed in Table 3 and plotted in Figure 8. Analysis on the effect of ice powder amount and gas mixture phases on SO_2 + CO_2 hydrate equilibrium conditions and the Gibbs phase rule application are also suitable to H_2S + CO_2 hydrate.

As shown in Figure 8, all of the measured equilibrium pressures for the H_2S + CO_2 hydrate are lower than those for the pure CO_2 hydrate. This proves that when H_2S is added to CO_2 the equilibrium pressure of CO_2 hydrate will decrease. It is also found that the higher the H_2S fraction, the larger the decrease from the CO_2 hydrate equilibrium pressure, as observed for SO_2 + CO_2 hydrate. In addition, we can see that the H_2S fraction increases when more hydrate dissociates at higher temperature. Again, as for SO_2, H_2S has a greater affinity for the hydrate phase than CO_2 and hence will concentrate in the hydrate. In the case of CO_2 storage, e.g., in depleted natural gas reservoirs under hydrate-forming conditions, residual H_2S will affect CO_2 hydrate formation. Small amounts of H_2S will affect the hydrate formation process favorably by lowering the equilibrium pressure required to form the hydrate. Larger quantities of H_2S will lower the CO_2 capacity of the hydrate and hence the reservoir, as H_2S

DOI: 10.1021/acs.iecr.5b00350
Ind. Eng. Chem. Res. 2015, 54, 5543−5549

competes favorably with CO_2 as hydrate guest. It will be important to determine the optimum amount of H_2S that will aid the hydrate formation process without significantly affecting the storage capacity.

Because both CSMGem and Multiflash can be used to predict the stability conditions of H_2S + CO_2 hydrate, the model predictions are also listed in Table 3 for comparison with the experimentally measured data. The absolute deviation percentage (ADP) is also listed. It can be seen that the Multiflash prediction is more accurate than that of CSMGem (6.88% versus 14.26% in total). In addition, the predictions for the lower H_2S fraction (1% H_2S + 99% CO_2 in feed gas experiment) are more accurate than those for the higher H_2S fraction (10.93% versus 19.81% for CSMGem, 5.10% versus 9.84% for Multiflash). The reported data in this work can be used to improve the prediction quality of CSMGem and Multiflash.

In summary, both SO_2 and H_2S can decrease the equilibrium pressure of CO_2 hydrate. A small amount of SO_2 or H_2S (for example, 1% mole fraction in the feed mixture) does not decrease the dissociation pressure very much. For the larger SO_2 or H_2S fractions, the pressure decrease becomes appreciably larger. Model predictions for the SO_2 + CO_2 hydrate and H_2S + CO_2 hydrate equilibrium conditions can be developed or improved based on the experimental data.

CONCLUSIONS

Dissociation conditions of CO_2 + SO_2 and CO_2 + H_2S mixture-formed hydrate were experimentally measured by the isochoric dissociation method. Excepting temperature and pressure, vapor phase composition in the equilibrium state is also reported in the equilibrium conditions. Both SO_2 and H_2S can decrease the equilibrium pressure of the CO_2 hydrate. Raman spectra of the SO_2 and H_2S containing hydrates were measured. It was found the peaks of SO_2 in the large and small cage are at 1147.1 and 1155.4 cm^{-1}, respectively; the peaks of H_2S in large and small cage are at 2594.0 and 2603.0 cm^{-1}, respectively.

AUTHOR INFORMATION

Corresponding Author

*E-mail: John.Ripmeester@nrc-cnrc.gc.ca. Tel: +1-613-993-2011. Fax: +1-613-998-7833.

Present Addresses

†L.C.: Center for Hydrate Research, Colorado School of Mines, Golden, CO 80401.

‡H.L.: College of Engineering, Peking University, Beijing 100871, China.

Notes

The authors declare no competing financial interest.

ACKNOWLEDGMENTS

We thank NRCan for the financial support of this study.

REFERENCES

(1) Corinne, L. Q.; Michael, R. R.; Josep, G. C.; Gregg, M. Trends in the source and sinks of carbon dioxide. *Nat. Geosci.* **2009**, *2*, 831.

(2) Yang, H.; Xu, Z.; Fan, M.; Gupta, R.; Slimane, R. B.; Bland, A. E.; Wright, I. Progress in carbon dioxide separation and capture: A review. *J. Environ. Sci. (Beijing, China)* **2008**, *20*, 14.

(3) Li, X.; Xia, Z.; Chen, Z.; Yan, K.; Li, G.; Wu, H. Gas hydrate formation process for capture of carbon dioxide from fuel gas mixture. *Ind. Eng. Chem. Res.* **2010**, *49*, 11614.

(4) Mohammadi, A. H.; Richon, D. Equilibrium data of sulfur dioxide and methyl mercaptan clathrate hydrates. *J. Chem. Eng. Data* **2011**, *56*, 1666.

(5) Beeskow-Strauch, B.; Schicks, J. M.; Spangenberg, E.; Erzinger, J. The influence of SO_2 and NO_2 impurities on CO_2 gas hydrate formation and stability. *Chem.—Eur. J.* **2011**, *17*, 4376.

(6) Daraboina, N.; Ripmeester, J. A.; Englezos, P. The impact of SO_2 on post combustion carbon dioxide capture in bed of silica sand through hydrate formation. *Int. J. Greenhouse Gas Control* **2013**, *15*, 97.

(7) Kim, S. H.; Huh, C.; Kang, S.; Kang, J. W.; Lee, C. S. Phase equilibria containing gas hydrate for carbon dioxide, sulfur dioxide, and water mixtures. *J. Chem. Eng. Data* **2013**, *58*, 1879.

(8) Sloan, E. D.; Koh, C. A. *Clathrate Hydrates of Natural Gases*, 3rd ed.; CRC Press: Boca Raton, FL, 2007; pp 4, 78.

(9) Selleck, F. T.; Carmichael, L. T.; Sage, B. H. Phase behavior in the hydrogen sulfide-water system. *Ind. Eng. Chem.* **1952**, *44*, 2219.

(10) Carroll, J. J.; Mather, A. E. Phase equilibrium in the system water-hydrogen sulphide: Hydrate-forming conditions. *Can. J. Chem. Eng.* **1991**, *69* (5), 1206.

(11) Ward, Z. T.; Deering, C. E.; Marriott, R. A.; Sum, A. K.; Sloan, E. D.; Koh, C. A. Phase equilibrium data and model comparisons for H_2S hydrates. *J. Chem. Eng. Data* **2015**, *60*, 403−408 DOI: 10.1021/je500657f.

(12) Robinson, D. B.; Hutton, J. M. Hydrate formation in systems containing methane, hydrogen sulphide and carbon dioxide. *J. Can. Pet. Technol.* **1967**, *6*, 6.

(13) Sun, C. Y.; Chen, G. J.; Lin, W.; Guo, T. M. Hydrate formation conditions of sour natural gases. *J. Chem. Eng. Data* **2003**, *48*, 600.

(14) Nohra, M.; Woo, T. K.; Alavi, S.; Ripmeester, J. A. Molecular dynamics Gibbs free energy calculations for CO_2 capture and storage in structure I clathrate hydrates in the presence of SO_2, CH_4, N_2, and H_2S impurities. *J. Chem. Thermodyn.* **2012**, *44*, 5.

(15) Adlsasmito, S.; Frank, R. J.; Sloan, E. D. Hydrates of carbon dioxide and methane mixtures. *J. Chem. Eng. Data* **1991**, *36*, 68.

(16) Chen, L.; Sun, C.; Nie, Y.; Sun, Z.; Yang, L.; Chen, G. Hydrate equilibrium conditions of (CH_4 + C_2H_6 + C_3H_8) gas mixtures in sodium dodecyl sulfate aqueous solutions. *J. Chem. Eng. Data* **2009**, *54*, 1500.

(17) Rodriguez-Carvajal, J. Recent developments of the program FullProf. *Commission on Powder Diffraction (IUCr) Newsletter* **2001**, *26*, 12.

(18) Buldakov, M. A.; Matrosov, I. I.; Petrov, D. V.; Tikhomirov, A. A. Raman gas-analyzer for analyzing environmental and technogenic gas media. *Atmos. Oceanic Opt.* **2012**, *25*, 298.

(19) Chen, L.; Lu, H.; Ripmeester, J. A. Raman spectroscopic study of CO_2 in hydrate cages. *Chem. Phys. Lett.*, submitted for publication.

(20) Anderson, A.; Savoie, R. Raman spectrum of crystalline and liquid SO_2. *Can. J. Chem.* **1965**, *43*, 2271.

(21) Brooker, M. H. Raman investigation of the structure of solid sulfur dioxide. *J. Mol. Struct.* **1984**, *112*, 221.

(22) Chazallon, B.; Focsa, C.; Charlou, J.; Bourry, C.; Donval, J. A comparative Raman spectroscopic study of natural gas hydrates collected at different geological sites. *Chem. Geol.* **2007**, *244*, 175.

(23) Hester, K. C.; Dunk, R. M.; White, S. N.; Brewer, P. G.; Peltzer, E. T.; Sloan, E. D. Gas hydrate measurements at Hydrate Ridge using Raman spectroscopy. *Geochim. Cosmochim. Acta* **2007**, *71*, 2947.

(24) Pimentel, G. C.; Charles, S. W. Infrared spectral perturbations in matrix experiments. *Pure Appl. Chem.* **1963**, *7*, 111.

(25) Subramanian, S.; Sloan, E. D. Trends in vibrational frequencies of guests trapped in clathrate hydrate cages. *J. Phys. Chem. B* **2002**, *106*, 4348.

DOI: 10.1021/acs.iecr.5b00350
Ind. Eng. Chem. Res. 2015, 54, 5543−5549